Article

Not peer-reviewed version

Molecular Composition of Exogenous Dissolved Organic Matter Regulates Dissimilatory Iron Reduction and Carbon Emissions in Paddy Soil

Haibo Wang , XiPeng Liu , Yuchen Shu , Gang Li , ChengLiang Sun , Davey Jones , YongGuan Zhu , Xianyong Lin *

Posted Date: 4 September 2024

doi: 10.20944/preprints202409.0323.v1

Keywords: Greenhouse gas emissions; Biochar; Dissimilatory iron reduction; C sequestration; Organic amendments; Soil microbiome

 doi:10.20944/preprints202409.0323.v1

Article

Molecular Composition of Exogenous Dissolved Organic Matter Regulates Dissimilatory Iron Reduction and Carbon Emissions in Paddy Soil

Hai-Bo Wang [1,2], Xi-Peng Liu [3], Yu-chen Shu [1], Gang Li [4], Cheng-Liang Sun [1], Davey L. Jones [2,5], Yong-Guan Zhu [1,6] and Xian-Yong Lin [1,*]

[1] MOE Key Laboratory of Environment Remediation and Ecological Health, College of Environmental and Resource Sciences, Zhejiang University, Hangzhou 310058, China
[2] School of Environmental and Natural Sciences, Bangor University, Bangor, Gwynedd, LL57 2UW, UK
[3] Labortoire d'Ecologie Microbienne, UMR5557, Centre national de la recherche scientifique (CNRS), Lyon, France
[4] Key Laboratory of Urban Environment and Health, Ningbo Urban Environment Observation and Research Station, Institute of Urban Environment, Chinese Academy of Sciences, Xiamen 361021, China
[5] Food Futures Institute, Murdoch University, Murdoch, WA, 6150, Australia
[6] State Key Laboratory of Urban and Regional Ecology, Research Center for Eco-Environmental Sciences, Chinese Academy of Sciences, Beijing 100085, China
* Correspondence: xylin@zju.edu.cn; Tel.: +86-571-88982476; Fax: +86-571-86971395

Abstract: Soil carbon (C) cycling under anoxic conditions is mechanistically linked to dissimilatory iron (Fe) reduction, which could be regulated by exogenous dissolved organic matter (DOM). However, the impact of complex exogenous DOM on soil microbial activity and C-Fe coupling in paddy soils remains underexplored. With a 100-day microcosm experiment, we determined that the molecular composition of DOM derived from organic fertilizers and biochar on paddy soil affects soil microbial community, Fe reduction, and C emissions. Our results indicated that biochar-DOM significantly promoted Fe reduction and accelerated CH_4 and CO_2 emissions, and organic manure-DOM increased soil CO_2 emissions, which was closely related to the molecular composition of exogenous DOM. DOM molecules with high aromaticity (AI_{mod}) and high DBE, including lignins-vascular plant-derived polyphenols, lignins-polycyclic aromatics (PA), and condensed aromatics-PA, promoted soil Fe reduction and CH_4 emissions by enriching soil Fe-reducing bacteria (FeRB), reducing methanotrophs, and facilitating r-strategists at the early stage of incubation. Conversely, DOMs with low AI_{mod}, low DBE and high H/C, such as lignins-highly unsaturated and phenolic compounds and proteins-aliphatic compounds, enhanced CO_2 emissions by facilitating recalcitrant C degradation and CH_4 oxidation at the late stage of incubation. In conclusion, our study highlights the importance of the molecular composition of DOMs derived from organic amendments in regulating soil Fe reduction and C emissions. The findings offer novel insights into the effective utilization of agricultural resources and the mitigation of soil C emissions.

Keywords: greenhouse gas emissions; biochar; dissimilatory iron reduction; C sequestration; organic amendments; soil microbiome

1. Introduction

Paddy soils are globally crucial carbon (C) pools, acting as the primary source of greenhouse gases, including CO_2 and CH_4. It is reported that paddy soils contain 39%-127% higher soil organic C (SOC) stocks compared to adjacent counterparts [1,2]. The storage of SOC in paddy soils is primarily benefit from intricate physical protection involving iron (Fe) mineral-organic matter aggregation, adsorption, and co-precipitation processes on Fe (oxyhydr) oxides [3,4]. Although significantly aiding in C sequestration, the cycling of soil Fe, such as Fe (III) reduction, can lead to C loss [5,6]. In

 doi:10.20944/preprints202409.0323.v1

the prevailing anaerobic conditions of paddy fields, Fe (III) serves as a crucial terminal electron acceptor for Fe-reducing bacteria (FeRB) [7,8] and thus can be reduced to Fe (II) through dissimilatory Fe reduction (DIR) [9]. The DIR process can account for up to 44% of SOC mineralization in anoxic soils [5], suggesting its critical role in controlling soil C sequestration and C emission [10,11].

Soil DIR and C emission processes are strongly influenced by many environmental factors, such as pH, oxygen content, soil organic matter. Dissolved organic matter (DOM) represents the most active component, regulating soil DIR processes and C emission processes through abiotic effects (e.g, combination, co-precipitation and complexation) and biotic (e.g, electron donor and shuttle) mechanisms [12,13]. For instance, DOM can abiotically increase Fe^{2+} production by over four times through complexation and its high electron exchange capacities under anaerobic conditions [14,15]. From the perspective of biotic factors, soil microbial communities, such as FeRB play a significant role in influencing soil DIR and C emission, and their community structure is closely linked to DOM compositions [7,16,17]. Labile DOM, such as simple sugars and amino acids, are readily metabolized by FeRB as an energy and electron donor [17,18]. Recalcitrant DOM, such as lignocellulosic residues, may require a more extensive microbial consortium and longer degradation times to support DIR [19]. The interaction between FeRB and CH_4-metabolizing microbes has frequently been reported [20–22]. Some FeRB can exacerbate CH_4 emissions by transferring electrons from *Geobacteraceae* to *Methanosarcina* with the help of geoconductors [20]. Conversely, other FeRB like *Clostridium* and *Bacillus* can promote Fe-dependent anaerobic oxidation of CH_4 or compete with methanogens for electrons, resulting in suppressed CH_4 production and increased CO_2 emissions [21,22]. Furthermore, microbial functions vary with the DOM composition, suggesting that potential existence of bacterial specialization for specific substrates [23]. For example, oligotrophic microorganisms (K-strategists) grow slowly and tend to utilize recalcitrant C (e.g., lignin), whereas eutrophic microorganisms (r-strategists) grow rapidly and exclusively use labile C sources (e.g., starch and hemicellulose) [24–26]. Nonetheless, the potential specialization of DOM by FeRB and C-metabolizing microbes remains unclear due to the broad chemo-diversity of DOM. These microbes may exhibit a preference for specific DOMs as energy sources, thereby regulating the DIR process and greenhouse gas production.

The applying of organic amendments, including organic fertilizer (e.g., manure and crop straw) and the biochar derived from them, is considered essential practice in agroecosystems for improving either soil fertility or soil C sequestration [27,28]. These practices can introduce substantial amounts of DOM into the soil. For example, long-term application of manure and crop straw increases the soil concentration of dissolved organic C (DOC) by 45.2% and 35.8%, respectively [29–31], whereas biochar-derived DOM contributes 13.4–25.3% of DOC in agricultural soils [32,33]. Previous studies have examined the impact of various fundamental C sources, such as glucose, starch, short-chain fatty acids, oxalate, and propionate, on the soil Fe redox process and C emissions [7,10,17,18]. In a recent study, ^{13}C-labeled DOM derived from bermudagrass was found to accelerate soil CO_2 emissions by 41-49% under hypoxic conditions, as it promoted Fe reduction and was strongly influenced by Fe phase crystallinity [5]. However, the relationship between the molecular composition of the organic amendment-derived DOM and FeRB, as well as its effect on soil DIR and C emissions are not known.

In this study, we conducted a microcosm experiment where we added DOMs derived from manure and crop straw and biochar of these organic fertilizers to the paddy soil. We hypothesized that different DOM molecules would selectively affect FeRB and other microbes, leading to differences in soil DIR and C emissions. This study aims to (1) investigate the effects of exogenous DOMs addition on soil DIR and C emissions; (2) elucidate the relationship between DOM compositions and FeRB and C-metabolizing microbes; and (3) identify specific DOM molecules strongly linked to soil DIR and C emissions, thereby aiding in the prediction of C emission risk and the agricultural waste utilization in paddy soils.

 doi:10.20944/preprints202409.0323.v1

2. Materials and Methods

2.1. Soil Sampling and Biochar Preparation

The soil samples used in this experiment were collected from the surface layer (0–20 cm) of a rice paddy field located in Si'an, Changxing County, Zhejiang Province, China (30°54′11″N, 119°37′26″E). The study site experiences a subtropical humid monsoon climate with an average annual temperature of 15.6°C and 1309 mm of precipitation. Prior to the experiment, the soil samples were homogenized by manually mixing and removing visible plant debris, rocks, and soil microfauna. Subsequently, the soil samples were air-dried and sieved using standard 2 mm screens. The soil samples in this area were classified as reddish paddy soil, and their physicochemical properties were presented in Supplementary Text S1. Two types of biochar were produced from manure and crop straw (rice) at a temperature of 600 ℃, respectively. The heating rate was set at 1℃ per minute, starting from 40℃, followed by 3 hours of continuous heating at the final temperature. Subsequently, the manure, crop straw, manure-biochar, and straw-biochar were sieved using 2 mm screens.

2.2. Soil Anaerobic Incubation and Measurements

Dry soil was mixed with sterile ultrapure water at a 1:2 ratio and pre-incubated at 25 °C for 7 days to eliminate the influence of native electron acceptors. After pre-incubation, 30 g of experimental soil (non-sterilized) was placed in a set of sterile 100 mL serum bottles. To elucidate the microbial response to DOM, the same amount of sterilized soil slurries prepared using gamma radiation at a dosage of 50 k Gray were placed in the serum bottles. Four treatments were established as follows: (1) soil slurries amended with different DOM; (2) sterilized soil slurries amended with different DOM; (3) soil slurries with sterile ultrapure water (CK); (4) sterilized soil slurries with sterile ultrapure water (MCK). The extraction process of DOM derived from organic manure, crop straw, manure-biochar, and crop-biochar is described in 2.3. The salt-free DOM was filtered using 0.22 μm membrane filters to eliminate microorganisms prior to their addition to the soil slurries. The concentration of dissolved organic C (DOC) in the salt-free DOM used in the experiments was diluted to 60 mg L^{-1}. Each serum bottle was filled with 60 mL of either DOM solution or ultrapure water. Subsequently, the bottles were sealed with sterile neoprene septa, capped with aluminum caps, and purged with Ar gas until an anaerobic environment was established. The anaerobic serum bottles were incubated in the dark at 25 °C for a duration of 100 days. The DOM derived from organic manure, crop straw, manure-biochar, and crop straw-biochar were referred to as OM-DOM, CS-DOM, OB-DOM, and CB-DOM, respectively, in the subsequent analyses. Soil slurries amended with OM-DOM, CS-DOM, OB-DOM, and CB-DOM were labeled as OM, CS, OB, and CB, respectively. Sterilized soil slurries amended with OM-DOM, CS-DOM, OB-DOM, and CB-DOM were designated as MOM, MCS, MOB, and MCB, respectively. Sterilized and unsterilized soil treatments with the addition of sterile ultrapure water were used as controls and named MCK and CK, respectively. The experiment comprised ten treatments (CK, OM, CS, OB, CB, MCK, MOM, MCS, MOB and MCB), each replicated four times and designed for sequential sample sacrifice.

Sets of bottles were sacrificed on days 3, 10, 30, 60, and 100. Each bottle was sampled by withdrawing 10 mL of headspace gas for CO_2 and CH_4 analyses, and 20 mL of homogenized suspension was transferred to a glovebox for Eh, pH, DOC, Fe-OM, and Fe species analyses. Soil pH and Eh were measured using a pH and Eh meter (Sartorius, Beijing, China) in a 1:5 (w/v) mixture without stirring the soil and water layer. Soil slurries from each treatment were collected, freeze-dried, and used for DOM extraction. Fe-OM was extracted using a solution of 0.27M trisodium citrate, 0.11M sodium bicarbonate, and 0.1M sodium dithionite (total ionic strength: 1.85 M) as described by Patzner, Mueller, Malusova, Baur, Nikeleit, Scholten, Hoeschen, Byrne, Borch, Kappler and Bryce [6]. DOC and Fe-OM concentrations were determined using a multi-N/C 2100S TOC-TN analyzer (Analytik Jena AG, Jena, Germany). CO_2 and CH_4 were quantified using a gas chromatography system (Trace 1300, Thermo Scientific, USA). Additionally, 1 mL suspension was withdrawn for investigating the changes in Fe species through sequential extraction [34]. Before use, all solutions

 doi:10.20944/preprints202409.0323.v1

were degassed with 99.9% Ar. Briefly, a 1 mL of homogenized slurry was sequentially extracted using 10 ml of 1 M $CaCl_2$, 0.5 M HCl, 5 M HCl, and 1.3 M HF with 1.8 M H_2SO_4 to obtain the following: (i) exchangeable Fe, (ii) surface-bound or complexed Fe and Fe in low-crystalline minerals (e.g., ferrihydrite, siderite, and green rust-like phases), (iii) highly crystalline Fe-bearing minerals (e.g., hematite), and (iv) Fe in silicates and clays. Fe^{2+}, Fe^{3+} and total Fe (TFe) concentrations were measured using a UV−vis spectrometer (Shimadzu UV2550) with the phenanthroline method.

2.3. DOM Extraction and Characterization

Dissolved organic matter derived from organic manure, crop straw, manure-biochar, straw-biochar and soil samples from each treatment were prepared as described in our previous work [35]. Briefly, the DOMs in these materials were extracted using sterile ultrapure water at a liquid / solid ratio of 10:1. The extraction process involved shaking the mixture on a horizontal shaker at 200 rpm for 24 hours. Afterwards, the supernatants were separated by centrifugation at 4000 rpm for 20 minutes and passed through a 0.45-μm cellulose acetate membrane. The DOM was desalted using solid-phase extraction cartridges (Bond Elut-PPL, Agilent, USA) and acidified ultrapure water (pH 2) to remove dissolved compounds other than DOMs, such as inorganic phosphorus. The concentration of dissolved organic C (DOC) in the DOMs were determined by measuring the concentration in the dialysate using a multi-N/C 2100S TOC-TN analyzer (Analytik Jena AG, Jena, Germany).

The molecular characteristics of organic amendment-DOM and soil DOM at day 60 were analyzed using a Bruker Apex Ultra Fourier transform ion cyclotron resonance (FT-ICR-MS) equipped with a 9.4 T superconducting magnet (Bruker, Billerica, MA, USA) at Research Center for Eco-Environmental Sciences, Chinese Academy of Sciences. The relevant details of the FT-ICR MS measurement are provided in Text S2. All detected compounds were classified into biochemical classes, including Lipid, protein, carbohydrates, unsaturated hydrocarbons, lignin, tannins, condensed aromatics, aliphatic compounds (Ali), highly unsaturated and phenolic compounds (HUP), vascular plant-dervied polyphenols (VP) and combustion-derived polycyclic aromatics (PA), following the classification described by Zhang, Lv, He, Cao, He, Zhao, Wang and Jiang [36] (Table S1).

2.4. Bacterial 16S rRNA Gene Amplification, Illumina Sequencing, and Data Analysis

DNA was extracted from fresh soil samples (0.5 g) using a FastDNA Spin Kit, following the manufacturer's instructions (MP Biomedical, Santa Ana, USA). The isolated DNA was eluted in 100 μL of TE buffer. The quality and quantity of the extracted DNA were checked using a NanoDrop 2000 spectrophotometer (NanoDrop Technologies, Wilmington, DE, USA). Subsequently, the DNA in the samples was stored at -80 ℃ until further sequencing. For the characterization of bacterial community structure and composition, DNA samples obtained from 124 soil samples were amplified using 515F (5′-GTGCCAGCMGCCGCGG-3′) and 907R (5′-CCGTCAATTCMTTTRAGTTT-3′) primers targeting the hypervariable V4–V5 region of the 16S rRNA gene [37]. The amplicons were then purified, mixed in equal amounts, and subsequently sequenced on an Illumina Hiseq 2500 platform at Novogene. The 16S rRNA gene sequences were processed using the QIIME2 pipeline (version 2022.4). The demultiplexed sequences were trimmed and denoised with DADA2 to infer Amplicon Sequence Variants (ASVs). Taxonomy was assigned to representative sequences using a 515F/907R taxonomy classifier through training (Naive Bayes classifiers based on the Silva 138 database). For comparability, the feature table of each sample was rarefied to a depth of 10,000 sequences.

2.5. Quantification of Gene Abundances

We measured 35 functional genes related to C cycling in each sample using high-throughput quantitative PCR-based SmartChip analysis (WaferGen Biosystems, Fremont, USA). The primer information and the qPCR procedures are provided in [38]. The relative abundances of the genes

 doi:10.20944/preprints202409.0323.v1

were calculated after the normalizations by the number of 16s rRNA gene copies. These 35 functional genes could be classified into four subtypes, including C-degradation (i.e., starch, hemicellulose, cellulose, chitin, pectin and lignin degradation), C-fixation, CH_4 production, and CH_4 oxidation.

2.6. Statistical Analysis

One-way analysis of variance with Tukey tests in IBM SPSS Statistics 20 (IBM Corp., Armonk, NY, USA) was conducted to identify significant differences between means at $P < 0.05$. The mean ± standard deviation of soil properties and DOM characteristics were determined. The relationships between soil properties and the relative abundance of bacterial genera were evaluated through Spearman's correlation analysis. All statistical analyses were performed using R v.4.0.4. Principal Coordinates Analysis (PCoA) of OTUs, based on Bray-Curtis distance matrices, was used to test the differences in the bacterial community between treatments. Network analyses were employed to investigate the interactions between microbial communities and DOM composition. Spearman correlations between DOM and soil microbes were analyzed at a significance level of $P < 0.05$ using the 'psych', 'reshape2', and 'pheatmap' packages. Only the strong and significant interactions were selected to be visualized ($|r| > 0.7$, $P < 0.05$). Gephi (version 0.9.6) was used to visualize network figures and derive relative network topological properties. The contributions of DOM molecules in different organic amendments to soil Fe-reducing bacteria and methanotroph were predicted using a Random Forest analysis.

3. Results

3.1. Soil Properties and C Emission

Upon the addition of DOM derived from various organic amendments, the pH of the soil slurry underwent immediate changes, ranging initially from pH 6.3 to 6.7 (Figure S1a). Initially, the pH rapidly increased within the first 10 days and then gradually stabilized for the remaining duration (Figure S1a). After anaerobic incubation, CB significantly increased soil pH, while OM significantly reduced it compared to CK ($P < 0.05$, Figure S1a). In contrast, the Eh values exhibited a substantial decrease from 250 mV during the initial 30-day incubation period, eventually stabilizing at equilibrium values ranging from 0 to -175 mV by the end of the incubation period (Figure S1b). OB, CB and CS significantly decreased Eh compared to CK treatment ($P < 0.05$, Figure S1b). Besides, the changes in pH and Eh values in non-sterilized soil were notably greater than those in sterilized soil ($P < 0.05$, Figure S1b).

The addition of DOM significantly boosted soil CH_4 and CO_2 emissions in non-sterilized soil compared to CK (Figure 1a-d). Biochar-DOM (OB and CB) significantly increased CH_4 emissions on day 3 and day 60 of incubation, as well as significantly elevated CO_2 emissions on day 3 and day 30 compared to CK ($P < 0.05$, Figure 1a-d). The OM treatment significantly raised CO_2 emissions on day 60 and 100 compared to other treatments ($P < 0.05$, Figure 1a, c). By the end of the incubation period, the cumulative CH_4 emissions were in the order of CB ≈ OB > CS ≈ CK > OM, and the cumulative CO_2 emissions were in the in the order of OM > OB ≈ CB ≈ CS > CK ($P < 0.05$, Figure 1b, d). The minor changes in CO_2 and CH_4 emissions in sterilized soil showed that microorganisms were the key drivers of C emissions (Figure 1a-d). Therefore, we measured the concentrations of dissolved organic C (DOC) and Fe bound organic C (Fe-OM) in non-sterilized soil. Compared to CK, the OM treatment significantly enhanced DOC during the initial 60 days and significantly increased Fe-OM concentrations on day 30 and 60 ($P < 0.05$, Figure 1e, f). OB and CB significantly increased DOC on day 3 and decreased Fe-OM concentrations on day 30 ($P < 0.05$, Figure 1e, f), while CS raised DOC on day 10 ($P < 0.05$, Figure 1e).

 doi:10.20944/preprints202409.0323.v1

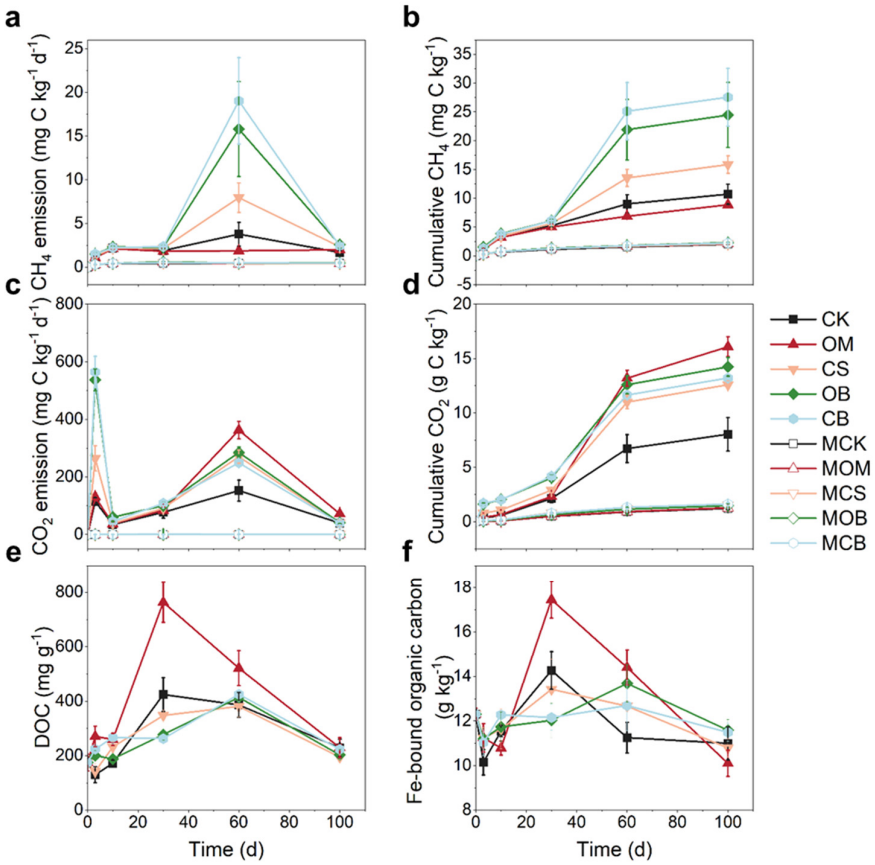

Figure 1. Soil carbon emission and carbon fraction after adding different dissolved organic matter (DOM). (a) CH_4 concentrations, (b) Cumulative CH_4 emission, (c) CO_2 concentrations, (d) Cumulative CO_2 emission, (e) Concentration of dissolved organic carbon (DOC) and (e) Concentration of Fe-bound organic carbon (Fe-OM) in the paddy soil after adding DOM. Error bars show standard deviations from quadruplicate measurements. OM, CS, OB and CB represent living soils with addition of the DOM derived from organic manure, crop straw, manure-biochar, and straw-biochar, respectively; MOM, MCS, MOB and MCB represent sterilized soils with addition of the DOM derived from organic manure, crop straw, manure-biochar, and straw-biochar, respectively.

3.2. Dissimilatory Fe reduction and Fe Species Transformation

The concentration of Fe^{2+} species increased gradually during the incubation period through DIR. The increase in Fe^{2+} was greater in most unsterilized treatments than in sterilized treatments, indicating the significance of soil microorganisms in DIR processes (Figure 2a-d). Various Fe^{2+} species exhibited different patterns of increase. For instance, $CaCl_2$-Fe^{2+} increased rapidly from days 3 to 30, 0.5M HCl-Fe^{2+} increased rapidly from days 3 to 60, and 5 M HCl-Fe^{2+} experienced slow growth from days 3 to 30, followed by rapid growth from days 30 to 60 (Figure 2a-c). In non-sterilized microcosms, $CaCl_2$-Fe^{2+}, 0.5 M HCl-Fe^{2+}, and 5 M HCl-Fe^{2+} significantly increased by 154.9–290.6 mg kg^{-1}, 510.8–2964.8 mg kg^{-1} and 1083.82–1240.2 mg kg^{-1}, respectively, during the incubation period (Figure 2a-c). In contrast, the HF-Fe^{2+} did not show a significant increasing trend during the incubation (Figure 2d). Biochar-DOM significantly increased $CaCl_2$-Fe^{2+} and 0.5 M HCl-Fe^{2+} contents by 48.5-72.8% and 117.5-164.0%, respectively, compared to CK ($P < 0.05$, Figure 2a, b). The CS treatment significantly increased the soil 0.5 M HCl-Fe^{2+}, while the OM treatment led to a significant decrease in 0.5 M HCl-Fe^{2+} contents by 48.9% compared with CK ($P < 0.05$, Figure 2a, b).

 doi:10.20944/preprints202409.0323.v1

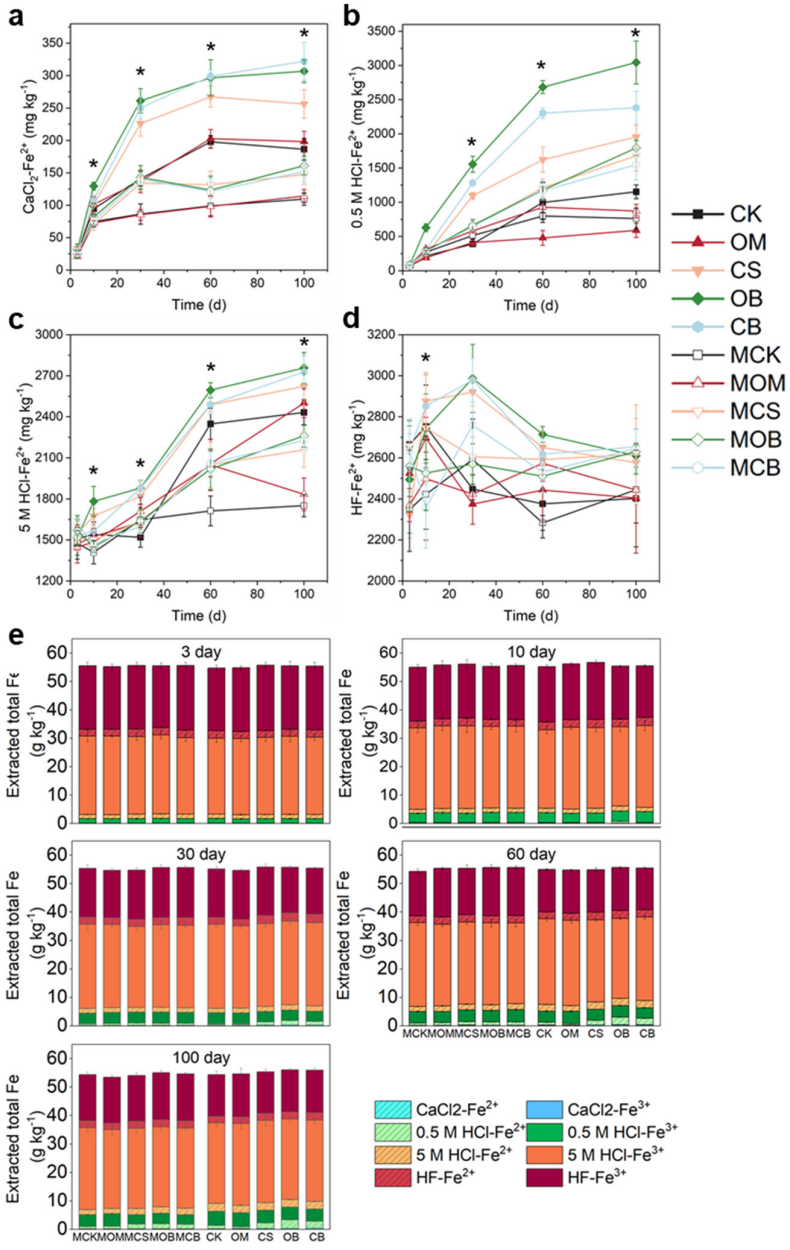

Figure 2. Changes in soil Fe^{2+} content and Fe species after adding different DOM. (a) $CaCl_2$-Fe^{2+}, (b) 0.5 M HCl-Fe^{2+}, (c) 5 M HCl-Fe^{2+}, (d) HF-Fe^{2+}, (e) Fe species in the paddy soils with addition of DOM. Comparisons between the sterilized and non-sterilized treatments denoted by asterisks were statistically significantly ($P < 0.05$). Error bars show standard deviations from quadruplicate measurements. The abbreviations of the treatments are shown in Figure 1.

Furthermore, the addition of DOM affected the variations of soil Fe species. $CaCl_2$-Fe and 0.5 M HCl-Fe contents significantly increased during the incubation period, whereas HF-Fe^{3+} content significantly decreased, regardless of the sterilized or non-sterilized treatments (Figure 2e). The magnitude of $CaCl_2$-Fe contents increased in the order of CB > OB > CS > OM ≈ CK during the incubation, while the magnitude of 0.5 M HCl-Fe contents increased in the order of OB ≈ OB > CS > OM ≈ CK ($P < 0.05$, Figure 2e). On day 60, 5 M HCl-Fe contents were highest in the CK treatment and lowest in the OB treatment (Figure 2e), while HF-Fe contents did not exhibit significant differences among treatments (Figure 2e).

 doi:10.20944/preprints202409.0323.v1

3.3. Soil Microbial Communities

The microbial community composition was investigated through Illumina sequencing based on 16S rRNA, comparing treatments with and without DOM addition. On the third day of incubation, the α-diversity (Chao1) was significantly lower in the CS, OB, and CB treatments compared to CK treatments ($P < 0.05$, Table S2). Whereas the α-diversity of all DOM addition treatments was significantly higher than that of the CK treatment on day 30 ($P < 0.05$, Table S2). During the initial 10 days of incubation, the highest *rrn* copy number of soil microbial communities was observed in biochar-DOM treatments, followed by CS treatment and OM treatment ($P < 0.05$, Table S3). Principal Coordinates Analysis (PCoA) revealed that the community structure diverged with different DOM additions. Biochar-DOM had a more significant impact on bacterial community structure compared to CS and OM (Figure 3a). However, these differences gradually decreased with incubation time, showing that the effect of DOM on soil microorganisms gradually diminished.

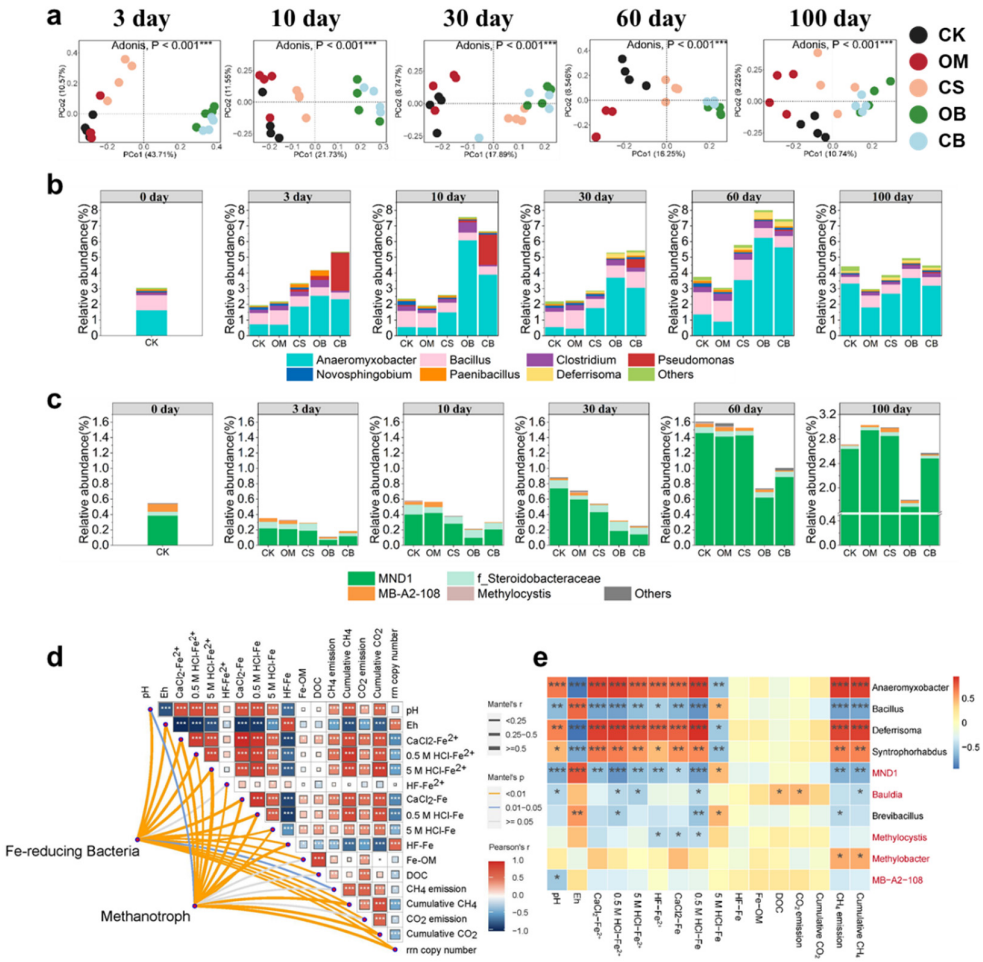

Figure 3. Changes in soil microbial composition within 100 days. (a) Principal coordinates analysis (PCoA) illustrating the impact of DOM addition on soil microbial communities. (b) Relative abundance of Fe-reducing bacteria (FeRB) (>0.01%), and (c) the relative abundance of methanotroph (>0.01%) at the genus level in paddy soils. (d) Pearson's correlation between soil biochemical properties matrix and the abundance of FeRB and methanotroph matrix during day 0-100 as determined by the Mantel test. (e) Correlation heatmap depicting the relationships among dominant FeRB (black labels), dominant methanotrophs (red labels), soil physicochemical properties, and C emission at Day 60. Different color intensities represent Pearson correlation coefficients. Significant correlations are indicated with asterisks: * $P < 0.05$, ** $P < 0.01$, *** $P < 0.001$. The abbreviations of the treatments are shown in Figure 1.

 doi:10.20944/preprints202409.0323.v1

The results at the phylum level revealed the presence of four dominant bacterial phyla in all treatments: *Proteobacteria*, *Bacteroidota*, *Acidobacteriota*, and *Myxococcota* (Figure S2). The CS, OB, and CB treatments significantly increased the relative abundance of r-strategists, including *Proteobacteria* (day 3-10), *Firmicutes* (day 10-100), and *Myxococcota* (day 10-100), compared to the CK treatment ($P < 0.05$, Figure S2a). In contrast, the OM treatment exhibited higher relative abundance of K-strategists compared to other DOM treatments (CS, OB, and CB), such as *Bacteroidota* (day 3-100), *Gemmatimonadota* (day 3-10) and *Verrucomicrobiota* (day 3-100) ($P < 0.05$, Figure S2a). At the family level (relative abundance >1%), biochar-DOM significantly increased the relative abundance of *Enterbacteriaceae* (day 3-10), *Anaeromyxobacteraceae* (day 3-60) and *Rhodocyclaceae* (day 10-100) ($P < 0.05$, Fig S2b).

Biochar-DOM treatment significantly increased the relative abundance of Fe-reducing bacteria (FeRB) compared to the other treatments during the initial 60 days ($P < 0.05$, Figure 3b). The OB treatment enriched *Anaeromyxobacter* (day 3-60), *Clostridium* (day 3-30), and *Deferrisoma* (day 30-60), and the CB treatment enriched *Anaeromyxobacter* (day 3-60), *Pseudomonas* (day 3-60), and *Deferrisoma* (day 30-60) ($P < 0.05$, Figure 3b). Similarly, the CS treatment increased the relative abundance of soil FeRB compared to CK, including *Anaeromyxobacter* (day 3-60), *Deferrisoma* (day 30-60), and *Paenibacillus* (day 3-10) ($P < 0.05$, Figure 3b). In contrast, the OM treatment decreased the abundance of soil FeRB compared to CK, including *Anaeromyxobacter* (day 30-100), *Novosphingobium* (day 10-100), and *Deferrisoma* (day 60-100) ($P < 0.05$, Figure 3b). Additionally, the biochar-DOM treatments significantly decreased the relative abundance of methanotrophs, particularly *MND1*, compared to the other treatments throughout the incubation period ($P < 0.05$, Figure 3c).

The relative abundance of FeRB and methanotrophs exhibited a strong correlation with Fe reduction and C emissions. Throughout the incubation period, FeRB had a significant impact on the increase of various Fe^{2+} species (except for HF-Fe^{2+}), the transformation of Fe species, and the emission of CH_4 and CO_2 ($P < 0.05$, Figure 3d). *Methanotrophs* also exerted a significant influence on the cumulative CH_4 and CO_2 ($P < 0.05$, Figure 3d). CH_4 and CO_2 emissions showed positive correlations with pH, Fe_{2+} species (except for HF-Fe^{2+}), $CaCl_2$-Fe, 0.5 M HCl-Fe, 5 M HCl-Fe, Fe-OM and DOC, while exhibiting negative correlations with Eh, HF-Fe and *rrn* copy number ($P < 0.05$, Figure 3d). The dominant FeRB species, such as *Anaeromyxobacter*, *Deferrisoma*, and *Syntrophorhabdus*, significantly promoted Fe reduction, the increase of low crystalline Fe ($CaCl_2$-Fe and 5 M HCl-Fe), and CH_4 emissions ($P < 0.05$, Figure 3e). Conversely, the dominant methanotroph species, *MND1*, exhibited a significant negative correlation with CH_4 emissions ($P < 0.05$, Figure 3e).

3.4. Abundance of Microbial C-Cycling Genes

Biochar-DOM significantly increased the abundance of labile C degradation genes compared to CK, such as *amyA*, *ipu*, *xylA* and *cex* at day 10, and *ipu*, *abfA*, *manB* and *xylA* at day 60 ($P < 0.05$, Figure 4a). Biochar-DOM also significantly enhanced abundance of CH_4 production genes (*pqq-mdh* and *mxaF*) compared to CK. OM and CS treatments significantly enhanced the abundance of lignin degradation genes compared to biochar-DOM treatments at day 10 and day 60, such as *glx*, *lig* and *mnp* ($P < 0.05$, Figure 4a). Besides, OM treatment significantly increased the abundance of CH_4 oxidation genes compared to other treatments at day 60 ($P < 0.05$, Figure 4a). The abundance of *xylA*, *frdA* and *amyA* were significantly positively correlated with 0.5 M HCl-Fe^{2+}, 0.5 M HCl-Fe, Fe-OM, CH_4 and CO_2 emission at day 10 ($P < 0.05$, Figure 4b). The abundance of *pmoA* was significantly positively correlated with CO_2 emission and the abundance of *pqq-mdh*, *xylA*, *smtA* and *abfA* were significantly positively correlated with CH_4 emission at day 60 ($P < 0.05$, Figure 4b). The abundance of *mmox* was significantly negatively correlated with CH_4 emission at day 60 ($P < 0.05$, Figure 4b).

 doi:10.20944/preprints202409.0323.v1

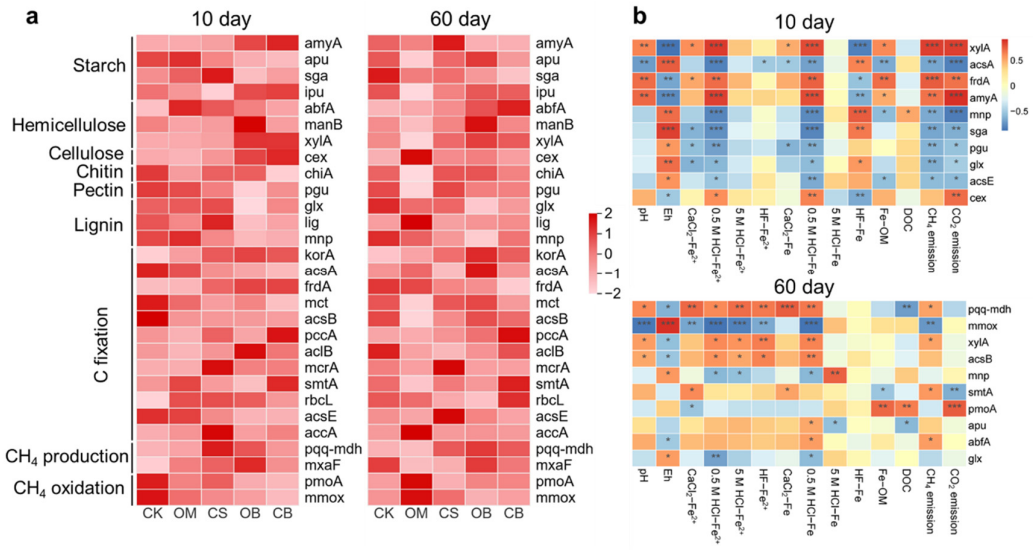

Figure 4. Response of soil C-cycling genes to exogenous DOM addition. (a) Relative abundance of soil C-cycling genes at Day 10 and 60 (Z-score transformed) (b) Correlation heatmap depicting the relationships among C-cycling genes, soil physicochemical properties, and C emission at Day 10 and 60. Different color intensities represent Pearson correlation coefficients. Significant correlations are indicated with asterisks: * $P < 0.05$, ** $P < 0.01$, *** $P < 0.001$. The abbreviations of the treatments are shown in Figure 1.

3.5. Characterization of Dissolved Organic Matter

The properties and molecular-level composition of DOM derived from organic amendments were significantly different. The electron donating capacity (EDC) values of DOM followed the order: CS-DOM > CB-DOM ≈ OM-DOM > OB-DOM ($P < 0.05$, Figure S4a). EDC was positively correlated with $CaCl_2$-Fe^{2+} and 0.5 M HCl-Fe^{2+} only in sterilized soil during the first 30 days ($P < 0.05$, Figure S4b, c). The proportions of combustion-derived polycyclic aromatics (PA) and vascular plant-derived polyphenols (VP) in biochar-DOM were significantly higher compared to OM-DOM and CS-DOM ($P < 0.05$, Figure S5a). Among the different types of DOMs, CB-DOM exhibited the highest abundance of lignins and condensed aromatics, while CS-DOM had the highest proportion of proteins, unsaturated hydrocarbons, and aliphatic compounds (Ali) (Figure S5a, b). OM-DOM contained the highest abundance of tannins and highly unsaturated and phenolic compounds (HUP) (Figure S5a, b). Elemental composition analysis of the classified formula groups revealed that CHO and CHON were the dominant components (Figure S5c). The proportions of CHO in CS-DOM and CB-DOM were significantly higher than those in OM-DOM and OB-DOM ($P < 0.05$, Figure S5c). OM-DOM and CS-DOM had a higher proportion of sulfur (S)-containing DOM compared to biochar-DOM ($P < 0.05$, Figure S5c). OM-DOM exhibited the highest proportion of nitrogen (N)-containing DOM (Figure S5c).

The intensity-weighted molecular parameters showed that biochar-DOM enhanced the recalcitrance of soil DOM at day 60. This was evidenced by higher values of O/C, DBE, aromaticity (AI_{mod}), and the proportion of recalcitrant components, as well as lower values of H/C in the OB and CB treatments compared to the CK treatment ($P < 0.05$, Figure S6a-f). The addition of biochar-DOM resulted in a significant increase in lignins, tannins, condensed aromatics, VP and PA ($P < 0.05$, Figure 5a, b). In contrast, manure-DOM led to a significant decrease in AI_{mod} and the proportion of recalcitrant components, while increasing the values of H/C and the proportion of labile compounds (lipids, protein and aliphatic compounds) compared to the CK treatment ($P < 0.05$, Figure 5a, b, Figure S6b, d). Besides, the CB treatment showed an increase in the relative proportions of CHON molecules and a decrease in the proportions of CHOS compared to the CK treatment ($P < 0.05$, Figure 5a). The

 doi:10.20944/preprints202409.0323.v1

OM treatment resulted in a significant increase in the relative proportions of CHOS molecules and a decrease in the proportions of CHO compared to the CK treatment ($P < 0.05$, Figure 5a).

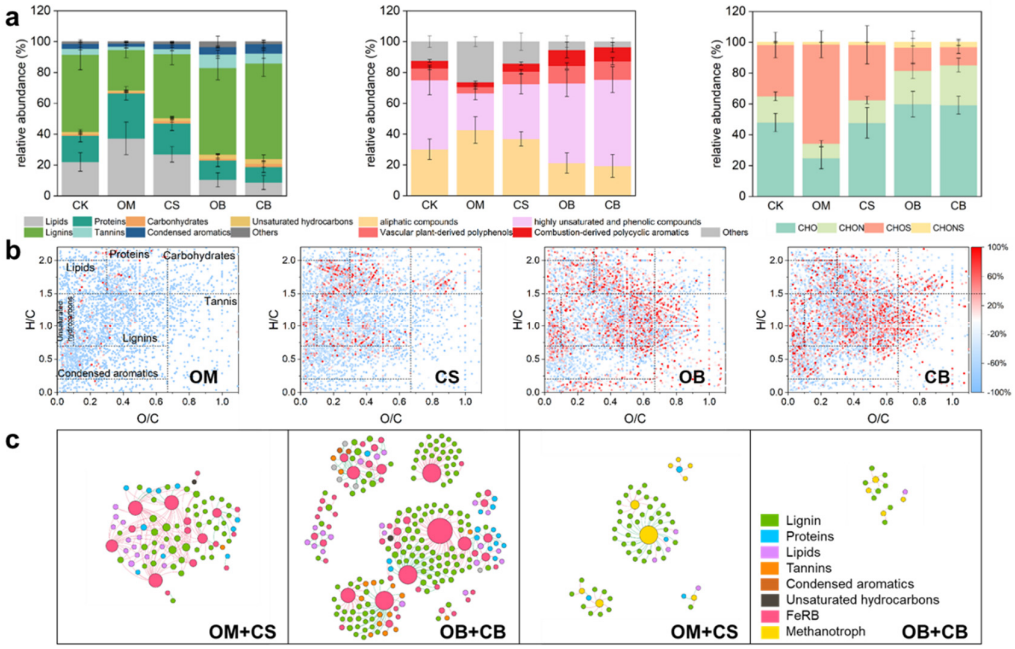

Figure 5. Response of soil DOM to exogenous DOM addition at Day 60. (a) Relative abundance (%) of van Krevelen diagram-derived classification classes and elemental composition formulae from the FT-ICR MS analysis of the soil DOM. Error bars show standard deviations from quadruplicate measurements. (b) The van Krevelen diagrams exhibiting the production and degradation of soil DOM molecules in different treatments compared to CK on the Day 60. The color of the DOM molecule represents an increase or decrease in the relative abundance in treatments compared to CK. (c) Network analyses for linking DOM molecules to FeRB (the two graphs on the left) and methanotroph (the two graphs on the right) under organic amendments and their biochar applications, respectively. Positive correlations are displayed in red and negative correlations were displayed in green. The size of each node is proportional to the number of connections (degree), and the color of each node indicates the classification of DOM and ASV. The abbreviations of the treatments are shown in Figure 1.

Network analysis showed the interactions between soil DOM molecules and bacterial communities on day 60. Biochar-DOM treatment strengthened the interactions between soil DOM and FeRB but weakened the interactions between DOM and methanotroph (Figure 5c). Anaeromyxobacter was predominant bacterial nodes in the DOM and FeRB network, mainly significantly positively correlated with lignin. In the DOM and methanotroph networks, MND1 and Methylocaldum were the dominant bacterial nodes. MND1 was positively correlated with lignin in all treatments (Figure 5c). Methylocaldum was negatively correlated with lignin compounds and positively correlated with lipids and proteins in OM and CS treatments (Figure 5c).

3.5. Specific DOM Molecules Associated with FeRB, Methanotrophs and Community r/K Strategy

The van Krevelen diagrams revealed distinct differences between the organic amendment-derived DOM molecules significantly correlated with Fe-reducing bacteria (FeRB) (blue) and those correlated with methanotrophs (orange) ($P < 0.05$, $r > 0$, Figure 6a). The DOM molecules that contributed the most to FeRB were lignins-VP, condensed aromatics-PA, and lignins-PA, whereas the DOM molecules that contributed the most to methanotrophs were lignins-HUP, tannins-HUP, and proteins-Ali (Figure 6b). In terms of elemental composition, CHO (59-66%) were dominant DOM

 doi:10.20944/preprints202409.0323.v1

molecules contributing to FeRB and methanotroph. The DOM molecules significantly contributing to FeRB were characterized by high AI_{mod} and DBE, including lignins-VP (32%), lignins-HUP (29%), and condensed aromatics-PA (16%). Conversely, the DOM molecules significantly contributing to methanotrophs had lower AI_{mod}, DBE and higher H/C and CHOS proportions, including lignins-HUP (64%) and aliphatic compounds (14%) ($P < 0.05$, Figure 6c and Table S4).

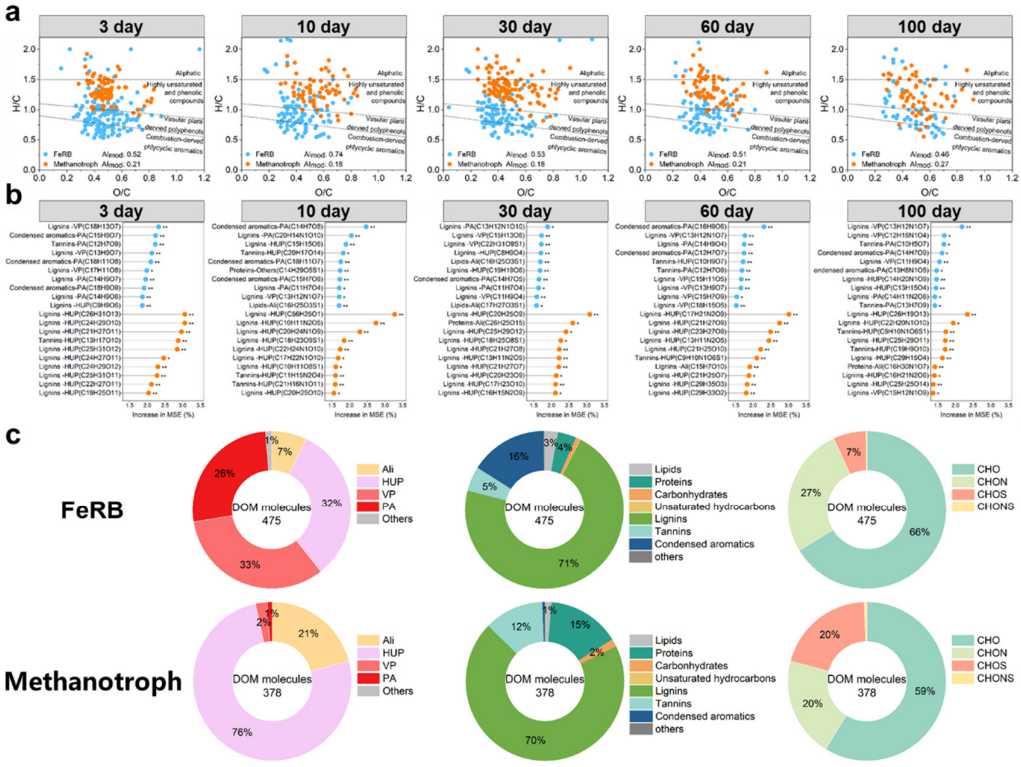

Figure 6. The exogenous DOM molecules significantly correlated with FeRB and methanotrophs. (a) The van Krevelen diagrams showing the the organic amendment-derived DOM molecules identified by Random Forest analysis for significant positive correlation with FeRB (blue) and methanotroph (orange). (b) Contribution of the top ten DOM molecules to the relative abundance of soil FeRB (blue) and methanotroph (orange) within 100 days by the Random Forest analysis. (c) Circle plots represent relative abundance of van Krevelen diagram-derived classification categories and elemental composition formulae of DOMs that significantly and positively correlated with relative abundance of FeRB and methanotroph within 100 days. Ali, aliphatic compounds; HUP, highly unsaturated and phenolic compounds; VP, vascular plant-derived polyphenols; PA, combustion-derived polycyclic aromatics.

Bacterial communities with a lower number of *rrn* operons tend to adopt a K-strategy (oligotrophy), while those with a higher *rrn* number tend to adopt an r-strategy (copiotrophy) [24,25], DOM molecules that shift communities towards adopting r-strategy (blue) and K-strategy (orange) were identified using Random Forest analysis. Lignins-VP (33%), lignins-HUP (29%), and condensed aromatics-PA (15%) were found to shift communities towards adopting r-strategy, while lignins-HUP (61%) and proteins-Ali (24%) favored the K-strategy ($P < 0.05$, Figure S7). Notably, the DOM molecules promoting the r-strategy exhibited higher AI_{mod} and DBE values, along with lower H/C and CHOS proportions compared to those that promote the K-strategy ($P < 0.05$, Table S4).

 doi:10.20944/preprints202409.0323.v1

4. Discussion

The soil C emission, DOM cycling, and dissimilatory Fe reduction (DIR) are intrinsically connected, yet the effect of molecular composition and properties of exogenous DOM on C emission and Fe reduction is still unclear. Our results demonstrate that soil CH_4 and CO_2 emissions are determined by multiple mechanisms that are regulated by DOM molecular properties. Our findings could provide a basis for the utilization of agricultural waste and predicting the risk of greenhouse gas emissions from paddy soils.

4.1. Exogenous DOM Promotes Microbial-Driven Fe Reduction in Paddy Soil

Our results indicate that soil Fe reduction is mainly affected by microbial activities (biotic factor) after the addition of exogenous DOM. This is supported from the significant higher Fe^{2+} content in the unsterilized soil added with DOM compared to that in sterilized soils. Another key evidence is that the electron-donating capacity (EDC) of exogenous DOM significantly correlated with the $CaCl_2$-Fe^{2+} and 0.5 M HCl-Fe^{2+} in sterilized soils whereas such correlation was not observed in unsterilized soils. This suggest that the EDC of DOM contributes to Fe reduction in an abiotic way (e.g., electron shuttling) [39,40], whereas soil microorganisms have a more significant impact on Fe reduction. Although most DOM (e.g., biochar-DOM and straw-DOM) significantly promote low-crystalline Fe reduction, manure-DOM significantly inhibits low-crystalline Fe reduction. This might be due to the high adsorption capacity of manure-DOM on soil Fe minerals [35,41]. Manure-DOM inhibits the DIR process by facilitating particle aggregation of Fe (III) minerals, blocking active Fe sites, and decreasing the surface charge of Fe (III) minerals [41–43]. These results indicate that different DOM could affect Fe reduction in various mechanisms.

Fe-reducing bacteria (FeRB) may primarily regulate the Fe reduction process in soil [13,44]. We found that exogenous DOM strongly affects the abundance of soil FeRB and the impact is more pronounced during the initial stage of incubation following DOM addition. Specifically, the elevated abundance of FeRB in OB, CB and CS treatments, along with the significant correlation between FeRB and Fe^{2+}, indicate that biochar-DOM and straw-DOM promote soil DIR by stimulating the proliferation of FeRB. Previous studies reported that biochar acted as a "geobattery" and "geoconductor", facilitating electron transfer between FeRB and Fe^{3+} minerals [20,45]. Our findings support the notion that biochar-DOM may play a comparable role. Moreover, the significant correlation between FeRB communities with the $CaCl_2$-Fe^{2+}, 0.5 M HCl-Fe^{2+} and 5 M HCl-Fe^{2+}, rather than HF-Fe^{2+}, suggests that the crystallinity of Fe phases greatly restricts the soil DIR process. This indicates that the microbe-driven Fe reduction could be constrained by the availability of Fe species and microbe-Fe interactions. Indeed, we found that the proportion of $CaCl_2$-Fe and 0.5 M HCl-Fe increased in the OB and CB treatments compared other treatments, suggesting that biochar-DOM promote the conversion of high-crystalline Fe phases into low-crystalline Fe phases.

To reveal the potential effect of DOM molecular composition on FeRB and Fe reduction, we evaluate the molecular-level association between soil bacterial communities and DOM molecules by employing network analysis and Random Forest analysis [16,46,47]. The increased complexity of network in biochar-DOM treatments suggests that biochar-DOM promotes the interactions between soil FeRB and DOM. Moreover, we identified that *Anaeromyxobacter* is the dominant FeRB in network and its abundance was significantly and positively correlated with lignin abundance, implying a mutually beneficial ecological niche for *Anaeromyxobacter* and lignin. This aligns with previous findings that *Anaeromyxobacter* may use lignins as respiratory electron donors and shuttles to transfer electrons to quinone moieties and secrete porin-cytochrome-like proteins, promoting Fe mineral reduction [48–50]. The Random Forest analysis further shows that lignins-VP, lignins-PA, and condensed aromatics-PA with high DBE and AI_{mod} contribute to the enrichment of soil FeRB. These recalcitrant macromolecular DOM may decompose slowly and serve as persistent electron donors for FeRB, reducing structural Fe (III) in (oxyhydr)oxides and clay minerals [20,50]. In terms of elemental composition, CHO compounds accounted for 66% of the appropriate C source for FeRB, while CHOS may not be suitable for FeRB enrichment. The reduction of S may compete with Fe reduction for electrons, thereby suppressing the soil DIR process in the OM treatment [51–53].

 doi:10.20944/preprints202409.0323.v1

Therefore, lignins-VP, lignins-PA, condensed aromatics-PA and CHO compounds in organic amendment-derived DOM may mainly promote soil Fe reduction through enrichment of FeRB.

4.2. Exogenous DOM Affects Soil C Emissions

This study shows that soil CH_4 and CO_2 emissions are significantly affected by exogenous DOM addition which is closely related to the microbe-driven Fe reduction. However, the underlying mechanisms of CH_4 and CO_2 emissions are different and are elaborated as below.

4.2.1. Exogenous DOM Regulates Soil CH_4 Emission

The addition of organic amendment-derived DOM significantly affects soil CH_4 emissions. Specifically, biochar-DOM significantly increases CH_4 emissions compared to CK, which can be primarily attributed to the promotion of CH_4 production and the inhibition of CH_4 oxidation. Firstly, the presence of highly AI_{mod} and high DBE DOM compounds in biochar-DOM, such as lignins-VP, lignins-PA, and condensed aromatics-PA, increased the abundance of soil FeRB and methanogens, including *Anaeromyxobacter*, *Deferrisoma* and *Methanobacterium*. These highly aromatic substances may act as a ground conductor to promote interspecies electron transfer from FeRB to methanogens, facilitating OM biodegradation and CH_4 emissions [13,20,54]. Indeed, our results showed an increase in abundance of CH_4 production genes and CH_4 emissions in biochar-DOM treatments which were significantly correlated with Fe^{2+} content, suggesting DIR process strongly promotes CH_4 produciton. Additionally, the significant positive correlations between soil $CaCl_2$-Fe, 0.5 M HCl-Fe content and CH_4 emissions suggests that low crystalline Fe species play an important role in promoting CH_4 emissions, which might be due to low crystalline Fe minerals (e.g., ferrihydrite) can produce more Fe^{2+}, greatly enhancing the activity of methanogenesis [55]. Secondly, CH_4 generation may be benefit from the degradation of soil C pool by microbial communities affected by substrate availability. Previous studies have reported that bacterial communities with fewer *rrn* operons tend to adopt K-strategy (oligotrophy) and are more efficient at mineralizing the recalcitrant C, whereas those with higher *rrn* number tend to adopt r-strategy (i.e., copiotrophy) and are more efficient at degrading labile C [24,25]. In the first 10 day of incubation, the microbial communities under DOM amendments, especially biochar-DOM, tend to be r-strategists, such as *Proteobacteria, Enterobacteriaceae and Firmicutes*. This promotes the degradation of starch, hemicellulose and cellulose by increasing the abundance of labile C degradation genes (*amyA, ipu, xylA* and *cex*) in biochar-DOM treatment, thereby producing hydrogen as a substrate for CH_4 production [56–58]. Besides, CH_4 emission from anaerobic paddy soil is the net result of CH_4 production and oxidation, and only a portion of produced CH_4 is actually emitted [59]. Biochar-DOM significantly decreased the relative abundance of methanotrophs compared to OM and CS treatments, such as *MND1* and *Bauldia*, and reduced the abundance of the *mmox* and *pmoA*, thereby inhibiting CH_4 oxidation. It may be attributed to the preference of methanotrophs for DOM compounds such as lignins-HUP, Tannins-HUP and Protein-Ali. In summary, high AI_{mod} and high DBE DOM molecules present in biochar-DOM, such as lignins-VP, lignins-PA and condensed aromatics-PA, promoted CH_4 emission by mediating DIR, enriching r-strategists and inhibiting CH_4 oxidation.

4.2.2. Exogenous DOM Affects Soil CO_2 Emission

Exogenous DOM addition significantly increased soil CO_2 emissions. Biochar-DOM accelerates CO_2 emissions, whereas OM treatments result in higher cumulative CO_2 emissions. This is potentially due to multiple mechanisms such as changes in the DIR process and microbial community composition. The DIR process could lead to Fe-bound OM release into soil solution and accelerated the mineralization of SOM by microorganisms [5]. This was supported by the strong correlation between CO_2 emission and the concentration of Fe-bound OM and DOC in this study. Additionally, the changed life history strategy of microbial communities can strongly influence CO_2 emissions. Our study suggests that biochar-DOM can stimulate the whole community toward adapting r-strategy and increase the abundance of labile C degradation genes (*amyA*, *xylA* and *cex*), thereby promoting

 doi:10.20944/preprints202409.0323.v1

rapid degradation of labile DOM and CO_2 emission during the early period of incubation. This situation leads to the accumulation of recalcitrant C in the soil (Figure 5a). Compared to biochar-DOM, manure/straw-DOM enrich more K-strategists and recalcitrant C degradation genes (*glx*, *lig* and *mnp*) that mineralize soil recalcitrant C into labile DOM (e.g., proteins, lipids and aliphatic compounds), thereby increasing soil DOC during the early period of incubation. The consequence is thus that soil DOM was more intensively degraded during the 30-60 days of the incubation, resulting in higher CO_2 emission in the OM treatment. Besides, the enrichment of methanotroph and CH_4 oxidation genes (pmoA and mmox) in OM treatment promotes the conversion of CH_4 to CO_2, further increasing CO_2 emissions. Briefly, high AI_{mod} and high DBE DOM compounds in biochar-DOM accelerates CO_2 emissions by DIR process and r-strategists, and low AI_{mod} and low DBE DOM compounds in OM-DOM result in more cumulative CO_2 emissions by recalcitrant C degradation and CH_4 oxidation.

Our results suggest that high AI_{mod} and high DBE DOM compounds (e.g., lignins-VP, lignins-PA and condensed-PA) promote Fe reduction and C release, thus enriching soil r-strategists with labile C degradation genes at the early stage, which seems contrary to findings under aerobic conditions [58]. This may be due to the fact that soil Fe-OM content (10-18 g C kg^{-1}) in this study was much higher than the input DOC (0.12 g C kg^{-1}) content, while the C released by soil Fe reduction under anaerobic conditions serves as the main C source for microorganisms, rather than exogenous DOM. Exogenous recalcitrant C in biochar (e.g., lignins-VP, lignins-PA, and condensed-PA) strongly promote Fe reduction and C release, greatly increasing the content of labile C and thus shifting the microbial community towards r-strategy. In contrast, low AI_{mod} and low DBE DOM compounds (lignins-HUP and proteins-Ali) in OM treatment hardly promote Fe reduction. Soil Fe minerals adsorb large amounts of C-nutrient and limit microbial nutrients [60,61], which increased microbial demand for available C [62], allowing K-strategists in OM treatment to degrade more recalcitrant C for nutrients and thus increasing CO_2 emissions. Despite this study providing evidence for this mechanism, it still needs to be investigated by further experiments.

4.3. Environmental Implications

Manure, crop straw, and biochar are frequently applied as soil amendments to enhance fertility, releasing significant DOM into the soil [28,46,56]. Our findings indicate that the addition of exogenous DOM markedly increases soil cumulative CH_4 and CO_2 emissions by 79% and 69%, respectively, compared to CK treatment. Given that CH_4 has 84-fold greater global warming potential compared to CO_2, the ratio of CH_4 to CO_2 emissions (CH_4 / CO_2) significantly influences the greenhouse effect [63]. This study suggests that the presence of biochar-derived DOM is more likely to elevate the soil CH_4 / CO_2 ratio (Figure S8), potentially exacerbating global warming risks.

Our findings demonstrate that molecular category and properties of DOM play a crucial role in regulating soil CH_4 and CO_2 emissions. Specifically, high AI_{mod} and high DBE DOM molecules, such as lignins-VP, lignins-PA and condensed aromatics-PA, promote CH_4 emission and accelerate CO_2 emissions by stimulating DIR, enriching r-strategists and inhibiting CH_4 oxidation. Low AI_{mod}, low DBE and high H/C DOMs, such as, lignins-HUP and proteins-Ali, promoted CO_2 emission through promoting recalcitrant C degradation and CH_4 oxidation. Therefore, understanding the molecular composition and characteristics of DOMs is essential when applying organic amendments like biochar to mitigate potential ecological impacts. While the effects of DOM components on soil Fe reduction and C emissions have been observed in microcosms, their impacts on field-scale CH_4 and CO_2 emissions across different soil types warrant further investigation. Additionally, studies suggest that DOMs containing diverse constituent elements may enhance soil microbial community diversity and nutrient cycling (e.g., N and P) [56,64,65]. However, the mechanism of DOM components affecting soil microbial communities and nutrient cycling remain unclear and require further study. In summary, our study emphasizes the importance of comprehending the molecular composition and potential functions of DOMs derived from organic amendments for effective utilization of agricultural wastes and soil C emission mitigation.

Supplementary Materials: The following supporting information can be downloaded at the website of this paper posted on Preprints.org.

Author Contributions: Haibo Wang: Visualization, Investigation, Methodology, Conceptualization, Resources, Writing—original draft, Writing—review & editing. **Xipeng Liu:** Visualization, Conceptualization, Resources, Writing—review & editing. **Yucheng Shu:** Formal analysis, Methodology. **Gang Li:** Resources, Writing—review & editing. **Chengliang Sun:** Conceptualization, Writing—review & editing. **Davey L. Jones:** Conceptualization, Writing—review & editing. **Yongguan Zhu:** Conceptualization, Writing—review & editing. **Xianyong Lin:** Conceptualization, Supervision, Project administration, Funding acquisition, Writing—review & editing.

Acknowledgments: This work was supported by the National Natural Science Foundation of China (42477335 and 42077088) and National Key Research and Development Program of China (2023YFD1902901). We thank Dr. Liang Ni (AES of Zhejiang University) for his help in soil sample collection.

Conflicts of Interest: The authors declare no competing financial interest.

References

1. Wu, D.; Ren, C.; Ren, D.; Tian, Y.; Li, Y.; Wu, C.; Li, Q. New insights into carbon mineralization in tropical paddy soil under land use conversion: Coupled roles of soil microbial community, metabolism, and dissolved organic matter chemodiversity. *Geoderma* **2023**, *432*. DOI: 10.1016/j.geoderma.2023.116393.
2. Chen, X.; Hu, Y.; Xia, Y.; Zheng, S.; Ma, C.; Rui, Y.; He, H.; Huang, D.; Zhang, Z.; Ge, T.; et al. Contrasting pathways of carbon sequestration in paddy and upland soils. *Global Change Biology* **2021**, *27* (11), 2478-2490. DOI: 10.1111/gcb.15595.
3. Chi, J.; Fan, Y.; Wang, L.; Putnis, C. V.; Zhang, W. Retention of soil organic matter by occlusion within soil minerals. *Reviews in Environmental Science and Bio/Technology* **2022**, *21* (3), 727-746. DOI: 10.1007/s11157-022-09628-x.
4. Wilhelm, R. C.; Lynch, L.; Webster, T. M.; Schweizer, S.; Inagaki, T. M.; Tfaily, M. M.; Kukkadapu, R.; Hoeschen, C.; Buckley, D. H.; Lehmann, J. Susceptibility of new soil organic carbon to mineralization during dry-wet cycling in soils from contrasting ends of a precipitation gradient. *Soil Biology and Biochemistry* **2022**, *169*. DOI: 10.1016/j.soilbio.2022.108681.
5. Chen, C.; Hall, S. J.; Coward, E.; Thompson, A. Iron-mediated organic matter decomposition in humid soils can counteract protection. *Nat Commun* **2020**, *11* (1), 2255. DOI: 10.1038/s41467-020-16071-5.
6. Patzner, M. S.; Mueller, C. W.; Malusova, M.; Baur, M.; Nikeleit, V.; Scholten, T.; Hoeschen, C.; Byrne, J. M.; Borch, T.; Kappler, A.; et al. Iron mineral dissolution releases iron and associated organic carbon during permafrost thaw. *Nat Commun* **2020**, *11* (1), 6329. DOI: 10.1038/s41467-020-20102-6.
7. Xu, J. X.; Li, X. M.; Sun, G. X.; Cui, L.; Ding, L. J.; He, C.; Li, L. G.; Shi, Q.; Smets, B. F.; Zhu, Y. G. Fate of Labile Organic Carbon in Paddy Soil Is Regulated by Microbial Ferric Iron Reduction. *Environ Sci Technol* **2019**, *53* (15), 8533-8542. DOI: 10.1021/acs.est.9b01323.
8. Ding, L. J.; Su, J. Q.; Xu, H. J.; Jia, Z. J.; Zhu, Y. G. Long-term nitrogen fertilization of paddy soil shifts iron-reducing microbial community revealed by RNA-(13)C-acetate probing coupled with pyrosequencing. *ISME J* **2015**, *9* (3), 721-734. DOI: 10.1038/ismej.2014.159.
9. Kögel-Knabner, I.; Amelung, W.; Cao, Z.; Fiedler, S.; Frenzel, P.; Jahn, R.; Kalbitz, K.; Kölbl, A.; Schloter, M. Biogeochemistry of paddy soils. *Geoderma* **2010**, *157* (1-2), 1-14. DOI: 10.1016/j.geoderma.2010.03.009.
10. Jeewani, P. H.; Ling, L.; Fu, Y.; Van Zwieten, L.; Zhu, Z.; Ge, T.; Guggenberger, G.; Luo, Y.; Xu, J. The stoichiometric C-Fe ratio regulates glucose mineralization and stabilization via microbial processes. *Geoderma* **2021**, *383*. DOI: 10.1016/j.geoderma.2020.114769.
11. Moore, O. W.; Curti, L.; Woulds, C.; Bradley, J. A.; Babakhani, P.; Mills, B. J. W.; Homoky, W. B.; Xiao, K.-Q.; Bray, A. W.; Fisher, B. J.; et al. Long-term organic carbon preservation enhanced by iron and manganese. *Nature* **2023**. DOI: 10.1038/s41586-023-06325-9.
12. Li, Y.; Gong, X. Effects of Dissolved Organic Matter on the Bioavailability of Heavy Metals During Microbial Dissimilatory Iron Reduction: A Review. In *Reviews of Environmental Contamination and Toxicology Volume 257*, de Voogt, P. Ed.; Springer International Publishing, 2021; pp 69-92.
13. Dong, H.; Zeng, Q.; Sheng, Y.; Chen, C.; Yu, G.; Kappler, A. Coupled iron cycling and organic matter transformation across redox interfaces. *Nature Reviews Earth & Environment* **2023**. DOI: 10.1038/s43017-023-00470-5.
14. Chen, C.; Meile, C.; Wilmoth, J.; Barcellos, D.; Thompson, A. Influence of pO(2) on Iron Redox Cycling and Anaerobic Organic Carbon Mineralization in a Humid Tropical Forest Soil. *Environ Sci Technol* **2018**, *52* (14), 7709-7719. DOI: 10.1021/acs.est.8b01368.
15. Han, R.; Wang, Z.; Lv, J.; Zhu, Z.; Yu, G. H.; Li, G.; Zhu, Y. G. Multiple Effects of Humic Components on Microbially Mediated Iron Redox Processes and Production of Hydroxyl Radicals. *Environ Sci Technol* **2022**, *56* (22), 16419-16427. DOI: 10.1021/acs.est.2c03799.

16. Li, X. M.; Chen, Q. L.; He, C.; Shi, Q.; Chen, S. C.; Reid, B. J.; Zhu, Y. G.; Sun, G. X. Organic Carbon Amendments Affect the Chemodiversity of Soil Dissolved Organic Matter and Its Associations with Soil Microbial Communities. *Environ Sci Technol* **2019**, *53* (1), 50-59. DOI: 10.1021/acs.est.8b04673.
17. Luo, D.; Li, Y.; Yao, H.; Chapman, S. J. Effects of different carbon sources on methane production and the methanogenic communities in iron rich flooded paddy soil. *Sci Total Environ* **2022**, *823*, 153636. DOI: 10.1016/j.scitotenv.2022.153636.
18. Khan, I.; Fahad, S.; Wu, L.; Zhou, W.; Xu, P.; Sun, Z.; Salam, A.; Imran, M.; Jiang, M.; Kuzyakov, Y.; et al. Labile organic matter intensifies phosphorous mobilization in paddy soils by microbial iron (III) reduction. *Geoderma* **2019**, *352*, 185-196. DOI: 10.1016/j.geoderma.2019.06.011.
19. Merino, C.; Kuzyakov, Y.; Godoy, K.; Jofre, I.; Najera, F.; Matus, F. Iron-reducing bacteria decompose lignin by electron transfer from soil organic matter. *Sci Total Environ* **2021**, *761*, 143194. DOI: 10.1016/j.scitotenv.2020.143194.
20. Yang, Z.; Sun, T.; Kleindienst, S.; Straub, D.; Kretzschmar, R.; Angenent, L. T.; Kappler, A. A coupled function of biochar as geobattery and geoconductor leads to stimulation of microbial Fe(III) reduction and methanogenesis in a paddy soil enrichment culture. *Soil Biology and Biochemistry* **2021**, *163*. DOI: 10.1016/j.soilbio.2021.108446.
21. Zhang, X.; Xie, M.; Cai, C.; Rabiee, H.; Wang, Z.; Virdis, B.; Tyson, G. W.; McIlroy, S. J.; Yuan, Z.; Hu, S. Pyrogenic Carbon Promotes Anaerobic Oxidation of Methane Coupled with Iron Reduction via the Redox-Cycling Mechanism. *Environmental Science & Technology* **2023**, *57* (48), 19793-19804. DOI: 10.1021/acs.est.3c05907.
22. Luo, D.; Yu, H.; Li, Y.; Yu, Y.; Chapman, S. J.; Yao, H. A joint role of iron oxide and temperature for methane production and methanogenic community in paddy soils. *Geoderma* **2023**, *433*. DOI: 10.1016/j.geoderma.2023.116462.
23. Moran, M. A.; Kujawinski, E. B.; Stubbins, A.; Fatland, R.; Aluwihare, L. I.; Buchan, A.; Crump, B. C.; Dorrestein, P. C.; Dyhrman, S. T.; Hess, N. J.; et al. Deciphering ocean carbon in a changing world. *Proceedings of the National Academy of Sciences* **2016**, *113* (12), 3143-3151. DOI: 10.1073/pnas.1514645113.
24. Klappenbach Joel, A.; Dunbar John, M.; Schmidt Thomas, M. rRNA Operon Copy Number Reflects Ecological Strategies of Bacteria. *Applied and Environmental Microbiology* **2000**, *66* (4), 1328-1333. DOI: 10.1128/AEM.66.4.1328-1333.2000 (acccessed 2024/06/11).
25. Wu, L.; Yang, Y.; Chen, S.; Jason Shi, Z.; Zhao, M.; Zhu, Z.; Yang, S.; Qu, Y.; Ma, Q.; He, Z.; et al. Microbial functional trait of rRNA operon copy numbers increases with organic levels in anaerobic digesters. *The ISME Journal* **2017**, *11* (12), 2874-2878. DOI: 10.1038/ismej.2017.135.
26. Trivedi, P.; Anderson, I. C.; Singh, B. K. Microbial modulators of soil carbon storage: integrating genomic and metabolic knowledge for global prediction. *Trends in Microbiology* **2013**, *21* (12), 641-651. DOI: 10.1016/j.tim.2013.09.005.
27. Luo, L.; Wang, J.; Lv, J.; Liu, Z.; Sun, T.; Yang, Y.; Zhu, Y.-G. Carbon Sequestration Strategies in Soil Using Biochar: Advances, Challenges, and Opportunities. *Environmental Science & Technology* **2023**, *57* (31), 11357-11372. DOI: 10.1021/acs.est.3c02620.
28. Kozjek, K.; Manoharan, L.; Urich, T.; Ahrén, D.; Hedlund, K. Microbial gene activity in straw residue amendments reveals carbon sequestration mechanisms in agricultural soils. *Soil Biology and Biochemistry* **2023**, *179*. DOI: 10.1016/j.soilbio.2023.108994.
29. Musadji, N. Y.; Lemée, L.; Caner, L.; Porel, G.; Poinot, P.; Geffroy-Rodier, C. Spectral characteristics of soil dissolved organic matter: Long-term effects of exogenous organic matter on soil organic matter and spatial-temporal changes. *Chemosphere* **2020**, *240*. DOI: 10.1016/j.chemosphere.2019.124808.
30. Laurent, C.; Bravin, M. N.; Crouzet, O.; Pelosi, C.; Tillard, E.; Lecomte, P.; Lamy, I. Increased soil pH and dissolved organic matter after a decade of organic fertilizer application mitigates copper and zinc availability despite contamination. *Science of The Total Environment* **2020**, *709*. DOI: 10.1016/j.scitotenv.2019.135927.
31. Bu, R.; Ren, T.; Lei, M.; Liu, B.; Li, X.; Cong, R.; Zhang, Y.; Lu, J. Tillage and straw-returning practices effect on soil dissolved organic matter, aggregate fraction and bacteria community under rice-rice-rapeseed rotation system. *Agriculture, Ecosystems & Environment* **2020**, *287*. DOI: 10.1016/j.agee.2019.106681.
32. Fu, H.; Liu, H.; Mao, J.; Chu, W.; Li, Q.; Alvarez, P. J. J.; Qu, X.; Zhu, D. Photochemistry of Dissolved Black Carbon Released from Biochar: Reactive Oxygen Species Generation and Phototransformation. *Environmental Science & Technology* **2016**, *50* (3), 1218-1226. DOI: 10.1021/acs.est.5b04314.
33. Sun, Y.; Xiong, X.; He, M.; Xu, Z.; Hou, D.; Zhang, W.; Ok, Y. S.; Rinklebe, J.; Wang, L.; Tsang, D. C. W. Roles of biochar-derived dissolved organic matter in soil amendment and environmental remediation: A critical review. *Chemical Engineering Journal* **2021**, *424*. DOI: 10.1016/j.cej.2021.130387.
34. Chen, N.; Fu, Q.; Wu, T.; Cui, P.; Fang, G.; Liu, C.; Chen, C.; Liu, G.; Wang, W.; Wang, D.; et al. Active Iron Phases Regulate the Abiotic Transformation of Organic Carbon during Redox Fluctuation Cycles of Paddy Soil. *Environ Sci Technol* **2021**, *55* (20), 14281-14293. DOI: 10.1021/acs.est.1c04073.

35. Li, K.; Bi, Q.; Liu, X.; Wang, H.; Sun, C.; Zhu, Y.; Lin, X. Unveiling the role of dissolved organic matter on phosphorus sorption and availability in a 5-year manure amended paddy soil. *Sci Total Environ* **2022**, *838* (Pt 1), 155892. DOI: 10.1016/j.scitotenv.2022.155892.
36. Zhang, Q.; Lv, J.; He, A.; Cao, D.; He, X.; Zhao, L.; Wang, Y.; Jiang, G. Investigation with ESI FT-ICR MS on sorbent selectivity and comprehensive molecular composition of landfill leachate dissolved organic matter. *Water Research* **2023**, *243*. DOI: 10.1016/j.watres.2023.120359.
37. Zhou, J.; Wu, L.; Deng, Y.; Zhi, X.; Jiang, Y. H.; Tu, Q.; Xie, J.; Van Nostrand, J. D.; He, Z.; Yang, Y. Reproducibility and quantitation of amplicon sequencing-based detection. *ISME J* **2011**, *5* (8), 1303-1313. DOI: 10.1038/ismej.2011.11.
38. Zheng, B.; Zhu, Y.; Sardans, J.; Penuelas, J.; Su, J. QMEC: a tool for high-throughput quantitative assessment of microbial functional potential in C, N, P, and S biogeochemical cycling. *Sci China Life Sci* **2018**, *61* (12), 1451-1462. DOI: 10.1007/s11427-018-9364-7 From NLM Medline.
39. Kugler, S.; Cooper, R. E.; Wegner, C. E.; Mohr, J. F.; Wichard, T.; Kusel, K. Iron-organic matter complexes accelerate microbial iron cycling in an iron-rich fen. *Sci Total Environ* **2019**, *646*, 972-988. DOI: 10.1016/j.scitotenv.2018.07.258.
40. Xu, S.; Adhikari, D.; Huang, R.; Zhang, H.; Tang, Y.; Roden, E.; Yang, Y. Biochar-Facilitated Microbial Reduction of Hematite. *Environmental Science & Technology* **2016**, *50* (5), 2389-2395. DOI: 10.1021/acs.est.5b05517.
41. Wang, H.-B.; Liu, X.-P.; Jin, B.-J.; Shu, Y.-C.; Sun, C.-L.; Zhu, Y.-G.; Lin, X.-Y. High-molecular-weight dissolved organic matter enhanced phosphorus availability in paddy soils: Evidence from field and microcosm experiments. *Soil and Tillage Research* **2024**, *240*. DOI: 10.1016/j.still.2024.106099.
42. Di Iorio, E.; Circelli, L.; Angelico, R.; Torrent, J.; Tan, W.; Colombo, C. Environmental implications of interaction between humic substances and iron oxide nanoparticles: A review. *Chemosphere* **2022**, *303* (Pt 2), 135172. DOI: 10.1016/j.chemosphere.2022.135172 From NLM Medline.
43. ThomasArrigo, L. K.; Vontobel, S.; Notini, L.; Nydegger, T. Coprecipitation with Ferrihydrite Inhibits Mineralization of Glucuronic Acid in an Anoxic Soil. *Environmental Science & Technology* **2023**, *57* (25), 9204-9213. DOI: 10.1021/acs.est.3c01336.
44. Kappler, A.; Bryce, C.; Mansor, M.; Lueder, U.; Byrne, J. M.; Swanner, E. D. An evolving view on biogeochemical cycling of iron. *Nature Reviews Microbiology* **2021**, *19* (6), 360-374. DOI: 10.1038/s41579-020-00502-7.
45. Liu, F.; Rotaru, A.-E.; Shrestha, P. M.; Malvankar, N. S.; Nevin, K. P.; Lovley, D. R. Promoting direct interspecies electron transfer with activated carbon. *Energy & Environmental Science* **2012**, *5* (10). DOI: 10.1039/c2ee22459c.
46. Ling, L.; Luo, Y.; Jiang, B.; Lv, J.; Meng, C.; Liao, Y.; Reid, B. J.; Ding, F.; Lu, Z.; Kuzyakov, Y.; et al. Biochar induces mineralization of soil recalcitrant components by activation of biochar responsive bacteria groups. *Soil Biology and Biochemistry* **2022**, *172*. DOI: 10.1016/j.soilbio.2022.108778.
47. Zhou, L.; Wu, Y.; Zhou, Y.; Zhang, Y.; Xu, H.; Jang, K.-S.; Dolfing, J.; Spencer, R. G. M.; Jeppesen, E. Terrestrial dissolved organic matter inputs drive the temporal dynamics of riverine bacterial ecological networks and assembly processes. *Water Research* **2024**, *249*. DOI: 10.1016/j.watres.2023.120955.
48. Shi, L.; Dong, H.; Reguera, G.; Beyenal, H.; Lu, A.; Liu, J.; Yu, H. Q.; Fredrickson, J. K. Extracellular electron transfer mechanisms between microorganisms and minerals. *Nat Rev Microbiol* **2016**, *14* (10), 651-662. DOI: 10.1038/nrmicro.2016.93.
49. Sheng, Y.; Dong, H.; Kukkadapu, R. K.; Ni, S.; Zeng, Q.; Hu, J.; Coffin, E.; Zhao, S.; Sommer, A. J.; McCarrick, R. M.; et al. Lignin-enhanced reduction of structural Fe(III) in nontronite: Dual roles of lignin as electron shuttle and donor. *Geochimica et Cosmochimica Acta* **2021**, *307*, 1-21. DOI: 10.1016/j.gca.2021.05.037.
50. Stern, N.; Mejia, J.; He, S.; Yang, Y.; Ginder-Vogel, M.; Roden, E. E. Dual Role of Humic Substances As Electron Donor and Shuttle for Dissimilatory Iron Reduction. *Environ Sci Technol* **2018**, *52* (10), 5691-5699. DOI: 10.1021/acs.est.7b06574.
51. Lovley, D. R. Syntrophy Goes Electric: Direct Interspecies Electron Transfer. *Annu Rev Microbiol* **2017**, *71*, 643-664. DOI: 10.1146/annurev-micro-030117-020420 From NLM Medline.
52. Kölbl, A.; Kaiser, K.; Thompson, A.; Mosley, L.; Fitzpatrick, R.; Marschner, P.; Sauheitl, L.; Mikutta, R. Rapid remediation of sandy sulfuric subsoils using straw-derived dissolved organic matter. *Geoderma* **2022**, *420*. DOI: 10.1016/j.geoderma.2022.115875.
53. Ma, Q.; Tang, S.; Pan, W.; Zhou, J.; Chadwick, D. R.; Hill, P. W.; Wu, L.; Jones, D. L. Effects of farmyard manure on soil S cycling: Substrate level exploration of high- and low-molecular weight organic S decomposition. *Soil Biology and Biochemistry* **2021**, *160*. DOI: 10.1016/j.soilbio.2021.108359.
54. Guo, H.; Chen, C.; Liang, W.; Zhang, Y.; Duan, K.; Zhang, P. Enhanced biomethane production from anthracite by application of an electric field. *International Journal of Coal Geology* **2020**, *219*. DOI: 10.1016/j.coal.2020.103393.

55. He, Z.; Zhu, Y.; Feng, J.; Ji, Q.; Chen, X.; Pan, X. Long-term effects of four environment-related iron minerals on microbial anaerobic oxidation of methane in paddy soil: A previously overlooked role of widespread goethite. *Soil Biology and Biochemistry* **2021**, *161*. DOI: 10.1016/j.soilbio.2021.108387.
56. Liu, X.; Wang, H.; Wu, Y.; Bi, Q.; Ding, K.; Lin, X. Manure application effects on subsoils: Abundant taxa initiate the diversity reduction of rare bacteria and community functional alterations. *Soil Biology and Biochemistry* **2022**, *174*. DOI: 10.1016/j.soilbio.2022.108816.
57. Willems, A. The Family Comamonadaceae. In *The Prokaryotes: Alphaproteobacteria and Betaproteobacteria*, Rosenberg, E., DeLong, E. F., Lory, S., Stackebrandt, E., Thompson, F. Eds.; Springer Berlin Heidelberg, 2014; pp 777-851.
58. McLeod, M. L.; Bullington, L.; Cleveland, C. C.; Rousk, J.; Lekberg, Y. Invasive plant-derived dissolved organic matter alters microbial communities and carbon cycling in soils. *Soil Biology and Biochemistry* **2021**, *156*. DOI: 10.1016/j.soilbio.2021.108191.
59. Hao, Q.; Wang, O.; Jiao, J.-Y.; Xiao, L.; Zhang, Y.; Li, W.-J.; Liu, F. Methylobacter couples methane oxidation and N2O production in hypoxic wetland soil. *Soil Biology and Biochemistry* **2022**, *175*. DOI: 10.1016/j.soilbio.2022.108863.
60. Duan, X.; Li, Z.; Li, Y.; Yuan, H.; Gao, W.; Chen, X.; Ge, T.; Wu, J.; Zhu, Z. Iron–organic carbon associations stimulate carbon accumulation in paddy soils by decreasing soil organic carbon priming. *Soil Biology and Biochemistry* **2023**, *179*. DOI: 10.1016/j.soilbio.2023.108972.
61. Cui, Y.; Moorhead, D. L.; Wang, X.; Xu, M.; Wang, X.; Wei, X.; Zhu, Z.; Ge, T.; Peng, S.; Zhu, B.; et al. Decreasing microbial phosphorus limitation increases soil carbon release. *Geoderma* **2022**, *419*. DOI: 10.1016/j.geoderma.2022.115868.
62. Nottingham, A. T.; Turner, B. L.; Stott, A. W.; Tanner, E. V. J. Nitrogen and phosphorus constrain labile and stable carbon turnover in lowland tropical forest soils. *Soil Biology and Biochemistry* **2015**, *80*, 26-33. DOI: 10.1016/j.soilbio.2014.09.012.
63. Hu, H.; Chen, J.; Zhou, F.; Nie, M.; Hou, D.; Liu, H.; Delgado-Baquerizo, M.; Ni, H.; Huang, W.; Zhou, J.; et al. Relative increases in CH4 and CO2 emissions from wetlands under global warming dependent on soil carbon substrates. *Nature Geoscience* **2024**. DOI: 10.1038/s41561-023-01345-6.
64. Wen, Z.; Shang, Y.; Song, K.; Liu, G.; Hou, J.; Lyu, L.; Tao, H.; Li, S.; He, C.; Shi, Q.; et al. Composition of dissolved organic matter (DOM) in lakes responds to the trophic state and phytoplankton community succession. *Water Res* **2022**, *224*, 119073. DOI: 10.1016/j.watres.2022.119073 From NLM Medline.
65. Tang, S.; Ma, Q.; Marsden, K. A.; Chadwick, D. R.; Luo, Y.; Kuzyakov, Y.; Wu, L.; Jones, D. L. Microbial community succession in soil is mainly driven by carbon and nitrogen contents rather than phosphorus and sulphur contents. *Soil Biology and Biochemistry* **2023**, *180*. DOI: 10.1016/j.soilbio.2023.109019.